Letter

Mesoscopic fluctuating domains in strontium titanate

Benoît Fauqué[1,*] Philippe Bourges,[2] Alaska Subedi,[3] Kamran Behnia,[4] Benoît Baptiste,[5]
Bertrand Roessli,[6] Tom Fennell,[6] Stéphane Raymond,[7] and Paul Steffens[8]

[1]*JEIP, USR 3573 CNRS, Collège de France, PSL Research University, 11, place Marcelin Berthelot, 75231 Paris Cedex 05, France*
[2]*Laboratoire Léon Brillouin, CEA-CNRS, Université Paris-Saclay, CEA Saclay, 91191 Gif-sur-Yvette, France*
[3]*CPHT, CNRS, Ecole Polytechnique, IP Paris, F-91128 Palaiseau, France*
[4]*Laboratoire de Physique et d'Étude des Matériaux (ESPCI Paris-CNRS-Sorbonne Université),*
PSL Research University, 75005 Paris, France
[5]*IMPMC-Sorbonne Université CNRS, 4, place Jussieu, 75005 Paris, France*
[6]*Laboratory for Neutron Scattering and Imaging, Paul Scherrer Institut, Villigen 5232, Switzerland*
[7]*Université Grenoble Alpes, CEA, IRIG, MEM, MDN, 38000 Grenoble, France*
[8]*Institut Laue-Langevin, 71 Avenue des Martyrs, 38042 Grenoble Cedex 9, France*

Spatial correlations between atoms can generate a depletion in the energy dispersion of acoustic phonons. Two well-known examples are rotons in superfluid helium and the Kohn anomaly in metals. Here we report on the observation of a large softening of the transverse acoustic mode in quantum paraelectric $SrTiO_3$ by means of inelastic neutron scattering. In contrast to other known cases, this softening occurs at a tiny wave vector implying spatial correlation extending over a distance as long as 40 lattice parameters. We attribute this to the formation of mesoscopic fluctuating domains due to the coupling between local strain and ferroelectric fluctuations. Thus, a hallmark of the ground state of insulating $SrTiO_3$ is the emergence of hybridized optical-acoustic phonons. Mesoscopic fluctuating domains may play a role in quantum tunneling, which impedes the emergence of a finite macroscopic polarization.

In solids and fluids the energy cost of an elastic modulation $\hbar\omega$ is set by its wave-vector q ($=\frac{2\pi}{\lambda}$ where λ is its wavelength). This relation is encoded in the phonon dispersion $\omega(q)$. For long wavelengths, this energy is low, and the phonon dispersion is linear in q, and the slope defines the sound velocity. When λ becomes comparable with the interatomic distance, the discreteness of the lattice in solids gives rise to saturation of ω and a standing wave with a zero group velocity. A few exceptions to this monotonic dispersion are known, such as superfluid ^{4}He [1] and metals displaying a Kohn anomaly in their phonon spectrum [2,3]. In the case of helium, a phonon branch dubbed a roton displays a minimum at finite q. Roton-like dispersion has been recently identified in other quantum fluids [4,5] and has been predicted to occur in chiral materials [6] or classical acoustic metamaterials [7]. Broadly speaking, the presence of a soft acoustic branch indicates a tendency towards local order driven either by correlations between atoms and/or to the proximity of an instability in the system.

In this Letter, we report on the observation of a large softening of the transverse acoustic (TA) mode by means of inelastic neutron scattering in $SrTiO_3$, a quantum paraelectric solid [8]. In contrast with other cases of roton-like dispersion, the softening occurs at a very small $q \approx 4 \times 10^{-2}$ Å^{-1},

pointing to the existence of mesoscopic fluctuating domains as wide as $\approx$16 nm.

Ferroelectric ordering at low temperature is aborted in $SrTiO_3$ by zero-point quantum fluctuations [9–11]. The large dielectric constant in this state has made $SrTiO_3$ one of the most widely used substrates for growing oxide heterostructures [12]. The bulk solid has recently become a subject of renewed fundamental interest [13]. The temperature dependence of the dielectric constant has been associated with quantum criticality [14–16]. The dilute superconducting ground state which emerges upon doping [17] and its interplay with ferroelectricity [18,19] has attracted much attention as well as the electronic transport properties of the dilute metal [20–26]. The phonon softening observed here introduces a novel ingredient to this picture and may play a key role in what sets the ground state of $SrTiO_3$ [15,27,28] apart. We track its origin to the coupling between a transverse acoustic branch and ferroelectric fluctuations driven by the strong anharmonic lattice dynamics.

Such as other perovskites, $SrTiO_3$ exhibits a cubic structure at high temperature [shown in Fig. 1(a)] that is distorted to a phase with a lower symmetry phase upon cooling. Two transverse phonon modes soften during this transition. The first one, a TA mode located at the R point of the Brillouin zone, attains zero frequency at $T_{AFD} = 105$ K. This is the well-studied AFD transition where two neighboring oxygen octahedra rotate in opposite directions as shown on Fig. 1(b). The second, a transverse optical mode located at the Γ point
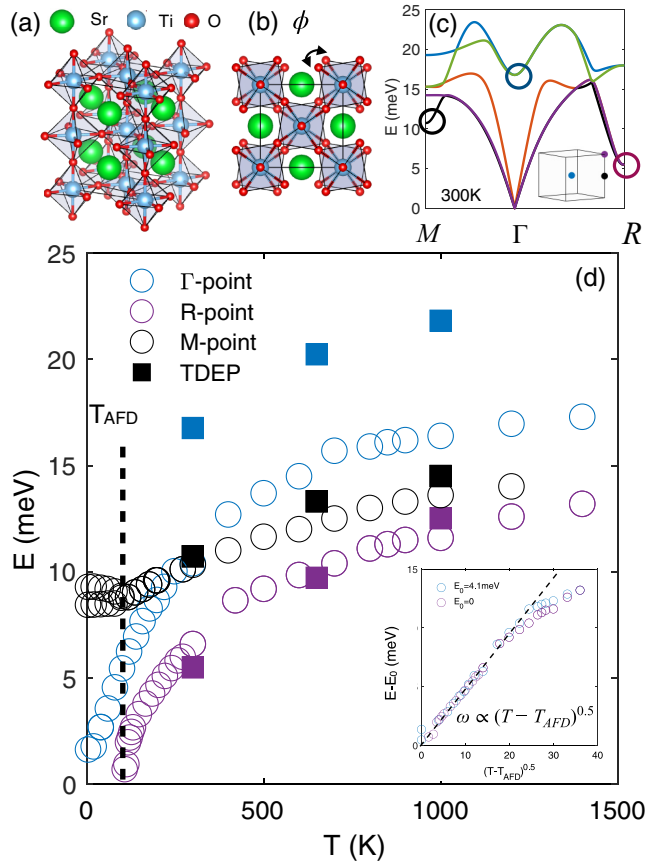
*benoit.fauque@espci.fr

FIG. 1. Soft phonons modes in SrTiO$_3$: (a) Lattice structure of SrTiO$_3$ the titanium atoms are in the center of oxygen polyhedras. (b) View along the c axis in the antiferrodistortive (AFD) phase below $T_{AFD} = 105$ K. (c) Phonon spectrum in the cubic phase of SrTiO$_3$ along the M-Γ-R direction at T = 300 K according to the temperature-dependent effective potential (TDEP) method (see Ref. [29]). The inset: Brillouin zone of the cubic phase of SrTiO$_3$. (d) Temperature dependence of the TO soft mode at Γ (blue), associated with the ferroelectric instability where cations and anions move in opposite ways and the two TA modes at R (purple) and M (black), associated with octahedra rotation of propagating wave-vectors $\mathbf{Q} = (0.5, 0.5, 0.5)$ and $(0.5, 0.5, 0)$, respectively. Open circle symbols are the experimental data (see Ref. [29] for the energy scans). Square closed symbols are the results found by the TDEP method. The inset: energy curves of the R mode and that of the Γ mode shifted down by 4.1 meV, and both plotted as a function of $(T - T_{AFD})^{0.5}$ where $T_{AFD} = 105$ K.

(TO$_\Gamma$) is associated with the motion of cations and anions in opposite ways, saturates at ≈ 2 meV at low temperature and gives rise to the quantum paraelectric behavior. Both modes have been separately investigated by inelastic neutron scattering [30,31], Raman [32,33], and optical spectroscopies [34,35]. We performed a systematic study of the phonon modes using inelastic neutron scattering at the Γ, R, and M points over a very large temperature range 4–1400 K. The obtained energy scans (shown in Ref. [29]) have been fitted with a damped harmonic oscillator (DHO). The energies of the fitted modes are reported in Fig. 1(d). The soft modes at Γ and R have the same temperature dependence. In contrast
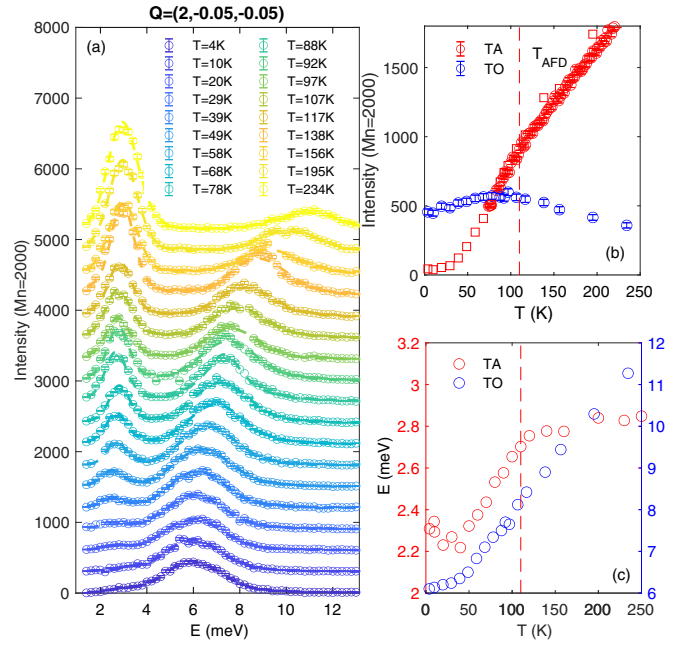

FIG. 2. TA-TO coupling in the quantum paraelectric phase of SrTiO$_3$: (a) Energy scans at $\mathbf{Q} = (2, -0.05, -0.05)$ for $T = 250$ K down to 4 K. Fits including a convolution with the experimental resolution are shown in dotted lines (see Ref. [29]). (b) Intensity of the acoustic (in red) and optical modes (in blue) as a function of temperature. (c) Energy position of the acoustic (red) and optical (blue) mode deduced from (a). We note a loss of intensity of the TA mode below T_{AFD} accompanied by a softening of the TA branch.

the M mode softens weakly and saturates at ~ 9 meV. When shifted by 4 meV, the energy of the Γ mode (ω_Γ) perfectly overlaps with the energy of the R mode (ω_R) on the whole temperature range [see the inset in Fig. 1(d)]. Given that the two modes belong to two distinct phonon branches [see Fig. 1(c)], this is remarkable. The two modes soften simultaneously from 1400 K following a mean-field-type temperature dependence [31,36] with the same prefactor. This observation implies that there is no primary mode driving the other one.

This experimental observation of the softening of the two phonon modes at Γ and R points contrasts with what is expected by density functional theory calculations based on the harmonic approximation. They predict unstable modes not only at the Γ and R points, but also at the M point [44] where two neighboring oxygen octahedra rotate in the opposite direction only on the (a)-(b) plane. This discrepancy between theory and experiment can be removed by including anharmonic effects in theory. This was performed with a TDEP method, recently developed and applied to the phonon spectrum of SrTiO$_3$ [45–49], which renormalizes the energies and the eigenvectors of the phonon spectrum. Square symbols in Fig. 1(d) show the energy position of these three modes found by our calculations at $T = 300$, 650, and 1000 K (see Ref. [29] for more details). There is excellent agreement for the R and M points and the relative temperature dependence of all three modes. At the Γ point the theoretical energy position overestimates ω_Γ, such as in previous calculations [45–48], suggesting that effects beyond phonon anharmonicity play a role in accurately describing this mode.
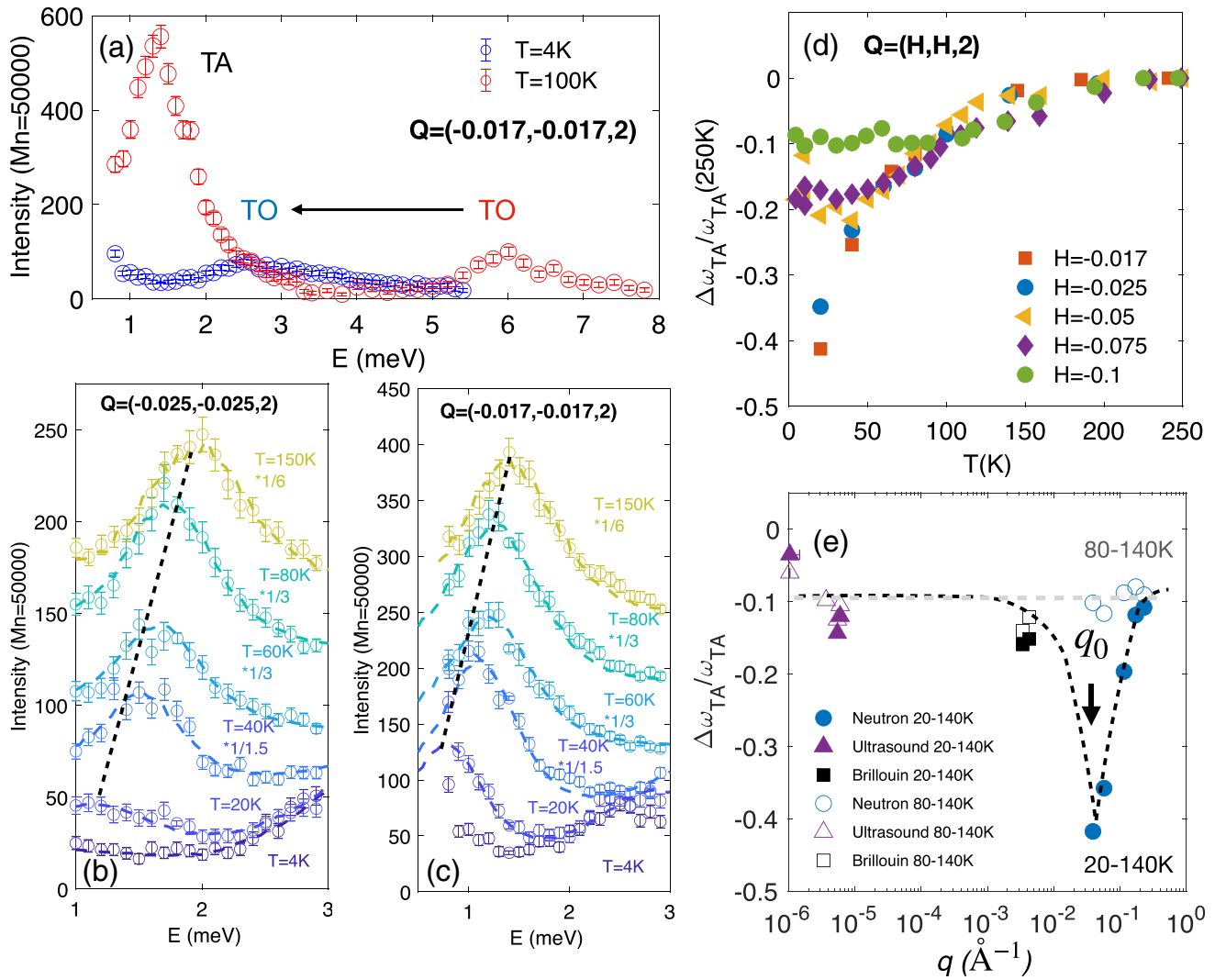
FIG. 3. Softening of the TA branch : (a) Energy scans at $\mathbf{Q} = (-0.017, -0.017, 2)$ for $T = 4$ K (in blue) and 100 K (in red). Low-energy scans at (b) $\mathbf{Q} = (-0.025, -0.025, 2)$ and (c) $\mathbf{Q} = (-0.017, -0.017, 2)$ from 150 down to 4 K. Curves are shifted and renormalized to underline the large softening shift of the TA branch. Fits with DHO including a convolution with the experimental resolution are shown in dotted lines (see Ref. [29]). (d) Normalized temperature dependence of the TA mode at different $\mathbf{Q}$ vectors. (e) Comparison of the magnitude of the softening of the TA branch with three different probes between 20 and 140 K: neutrons (this Letter), ultrasound [37–41], and Brillouin [42,43]. Note the horizontal logarithmic scale.

A second manifestation of the anharmonicity at work in SrTiO$_3$ occurs at low temperature. Two peaks are visible in the energy scan at $\mathbf{Q} = (2, -0.05, -0.05)$ [see Fig. 2(a)]. They correspond to the TA (corresponding to the elastic modulus c_{44}) and the TO$_\Gamma$ modes. As the temperature decreases, the softening of the TO$_\Gamma$ is accompanied by a dramatic loss of intensity of the acoustic branch. This effect, discovered more than 50 yr ago [31], is a consequence of hybridization between the TO$_\Gamma$ and TA modes [50]. In Landau's framework of phase transitions, this is the result of coupling between the strain and the gradient of fluctuations in the electric polarization [51]. Only recently, it has been explained by a first-principles approach invoking anharmonic coupling between the renormalized phonons [48].

Our systematic study of the temperature and $\mathbf{Q}$ dependence (shown in Figs. 2 and 3) reveals two new facts. First, the loss

of intensity is enhanced below T_{AFD} [see Fig. 2(b)]. Second, and most importantly, it is accompanied by a large phonon softening of the TA mode at a finite low Q vector. Measurements at lower $\mathbf{Q}$ [see Figs. 3(a)–3(c)] show that the loss of intensity affects the whole TA branch. However, softening is largest at lower $\mathbf{Q}$. Figure 3(d) shows the temperature dependence of the normalized amplitude of the softening, $\frac{\Delta\omega_{TA}}{\omega_{TA}(250\,\mathrm{K})} = \frac{\omega_{TA}(T)-\omega_{TA}(250\,\mathrm{K})}{\omega_{TA}(250\,\mathrm{K})}$ at $\mathbf{Q} = (H, H, 2)$ for $H = -0.017$ to -0.1. At $H = -0.1$ and $T = 20$ K, the softening was found to be about 10%, in agreement with previous measurements [31,43,48,52]. As H goes to zero, $\frac{\Delta\omega_{TA}}{\omega_{TA}(250\,\mathrm{K})}$ increases up to 0.4 at $H = -0.017$, the lowest $\mathbf{Q}$ where the TA branch could be measured in this Letter, see Ref. [29].

Interestingly, this result contrasts with the elastic constant measured at lower energies by the ultrasound technique (in the range of 10–100 MHz) [37–41] and Brillouin spectroscopy (in
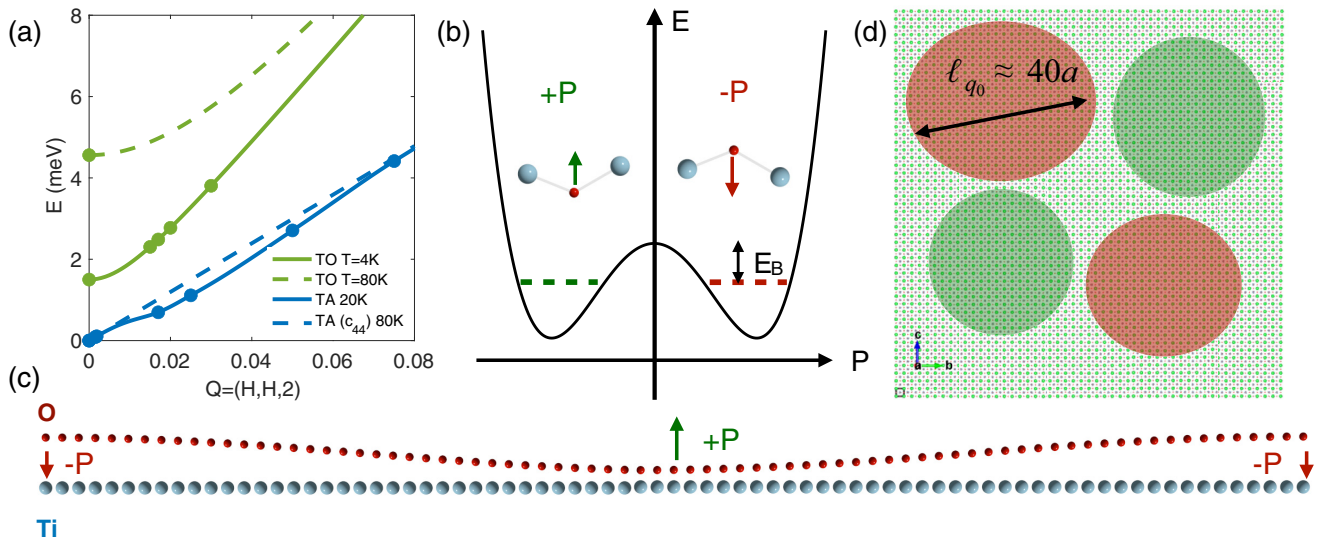
FIG. 4. Ground state of the quantum paraelectric $SrTiO_3$: (a) Dispersion of the TO (green) and TA (blue) modes at high (dotted lines) and low (full lines) temperature. The TA dispersion at $T = 80$ K assumes a constant sound velocity, $v_{44} = 4800$ ms^{-1} [38]. The TA dispersion at $T = 20$ K is deduced from the softening (dotted line) shown in Fig. 3(e). (b) Sketch of the free energy vs polarization: the long-range polarized order is not stabilized due to tunneling processes between the lowest-energy levels (dashed red and green lines) of the double-well potential. The energy barrier between the two energy levels is labeled E_B. (c) Sketch of a transverse elastic deformation over a length scale of $\ell_0 = \frac{2\pi}{q_0}$ as wide as 40 unit cells along (1,0,0). (d) This leads to fluctuating polarized domains of mesoscopic size of both signs.

the range of 20 GHz) [42,43,53]. Figure 3(e) shows the magnitude of the softening between 20 and 140 K (closed symbols) and between 80 and 140 K (open symbols) as a function of the q values ($=\omega/v_{44}$ where v_{44} is the sound velocity of the c_{44} mode) probed using those three techniques. Both ultrasound and Brillouin measurements show a sharp drop of v_{44} of 10% at T_{AFD}. Below T_{AFD}, a smooth and weak variation of about a few percent has been detected, in contrast with the 40% drop observed by neutron scattering.

Figure 3(e) implies that the softening of the TA mode upon cooling is most prominent at a finite $q_0 \approx 0.04$ Å^{-1} below T_{AFD} (see the dashed lines linking the three sets of low-temperature data). Note that one cannot exclude that the softening occurs at a q vector below our lowest data point and above what is resolved by Brillouin scattering, meaning that $\ell_0 = \frac{2\pi}{q_0}$ could be larger. In any case, the data imply the existence of spatial correlation on a length scale of, at least, $\ell_{q_0} \simeq 40a \approx 16$ nm where $a = 0.39$ nm is the lattice parameter. The softening of the TO_Γ is, therefore, accompanied by structural fluctuations extending over mesoscopic distances. We note that a similar softening can be found in $KTaO_3$ [50] around $q_0 \approx 0.2$ Å^{-1} pointing to the domain size five times shorter than in $SrTiO_3$.

Are these fluctuating domains intrinsic? In an extrinsic scenario, the length scale would require a defect density of 2×10^{17} cm^{-3} in our undoped $SrTO_3$ samples. Such a large concentration is unlikely since, with controlled doping, one can attain a carrier concentration much less than this and detect their corresponding quantum oscillations [17]. Therefore, our observation calls for an intrinsic mechanism invoking coupling between two transverse modes. Such a scenario was put forward as early as 2007 by Bussmann-Holder *et al.* and co-workers [54], who found that coupling between the TO_Γ and TA mode generates dynamical polarizability and ferroe-

lastic clusters. However, the length scale calculated down to $\approx$40 K is ten times shorter than the one observed by our experiment. A concrete evidence of the TO/TA coupling is detected through the increase in the phonon linewidth of the TA and TO modes that accompany the TA softening at low temperature (see Ref. [29]).

Up to now, the quantum paraelectric regime of $SrTiO_3$ was believed to be only driven by the soft TO_Γ mode [8–11]. In this picture, the ferroelectric order is aborted due to quantum tunneling between two zero-point energy levels (when $k_BT \ll E_B$, where E_B is the barrier energy) associated with two adjacent titanium oxygen bonds [see Fig. 4(b)]. Our result reveals a missing ingredient to this picture. The ground state of $SrTiO_3$ is formed by a hybridized optical-acoustic phonon mode where quantum fluctuations are accompanied by fluctuating domains of mesoscopic length. The vanishing of average polarization occurs, thus, in the context of quantum tunneling processes involving about 10^5 ($\approx 40^3$) atomic unit cells acting cooperatively as sketched in Fig. 4(c). This state can be viewed as an instanton liquid where thanks to dynamic clusters, despite zero average polarization notwithstanding, the mean square of polarization remains finite and may even increase with decreasing temperature [55].

Hybridization between optical and acoustic phonons reported here appears essential for understanding the unusual thermal conductivity [56], the sizable thermal Hall effect [57], the temperature dependence of the electric permittivity [14,15], and the dynamics of structural domains [58] of $SrTiO_3$. Our results would also impact the ongoing discussion on the origin of the superconductivity in lightly doped $SrTiO_3$. Coupling between the electrons and the TO_Γ mode plays a key role in a number of theoretical scenarios [21,22,26]. We have shown that a hybridized TO_Γ-TA phonon mode is to be taken

into account and may even change the understanding of the ground state of quantum paralectrics [59].

[1] D. G. Henshaw and A. D. B. Woods, Phys. Rev. **121**, 1266 (1961).

[2] W. Kohn, Phys. Rev. Lett. **2**, 393 (1959).

[3] B. Renker, H. Rietschel, L. Pintschovius, W. Gläser, P. Brüesch, D. Kuse, and M. J. Rice, Phys. Rev. Lett. **30**, 1144 (1973).

[4] H. Godfrin, M. Meschke, H.-J. Lauter, A. Sultan, H. M. Böhm, E. Krotscheck, and M. Panholzer, Nature (London) **483**, 576 (2012).

[5] L. Chomaz, R. M. W. van Bijnen, D. Petter, G. Faraoni, S. Baier, J. H. Becher, M. J. Mark, F. Wächtler, L. Santos, and F. Ferlaino, Nat. Phys. **14**, 442 (2018).

[6] J. Kishine, A. S. Ovchinnikov, and A. A. Tereshchenko, Phys. Rev. Lett. **125**, 245302 (2020).

[7] Y. Chen, M. Kadic, and M. Wegener, Nat. Commun. **12**, 3278 (2021).

[8] K. A. Müller and H. Burkard, Phys. Rev. B **19**, 3593 (1979).

[9] T. Schneider, H. Beck, and E. Stoll, Phys. Rev. B **13**, 1123 (1976).

[10] D. Shin, S. Latini, C. Schäfer, S. A. Sato, U. De Giovannini, H. Hübener, and A. Rubio, Phys. Rev. B **104**, L060103 (2021).

[11] T. Esswein and N. A. Spaldin, Phys. Rev. Res. **4**, 033020 (2022).

[12] P. Zubko, S. Gariglio, M. Gabay, P. Ghosez, and J.-M. Triscone, Annu. Rev. Condens. Matter Phys. **2**, 141 (2011).

[13] C. Collignon, X. Lin, C. W. Rischau, B. Fauqué, and K. Behnia, Annu. Rev. Condens. Matter Phys. **10**, 25 (2019).

[14] S. E. Rowley, L. J. Spalek, R. P. Smith, M. P. M. Dean, M. Itoh, J. F. Scott, G. G. Lonzarich, and S. S. Saxena, Nat. Phys. **10**, 367 (2014).

[15] M. J. Coak, C. R. S. Haines, C. Liu, S. E. Rowley, G. G. Lonzarich, and S. S. Saxena, Proc. Natl. Acad. Sci. USA **117**, 12707 (2020).

[16] P. Chandra, G. G. Lonzarich, S. E. Rowley, and J. F. Scott, Rep. Prog. Phys. **80**, 112502 (2017).

[17] X. Lin, Z. Zhu, B. Fauqué, and K. Behnia, Phys. Rev. X **3**, 021002 (2013).

[18] C. W. Rischau, X. Lin, C. P. Grams, D. Finck, S. Harms, J. Engelmayer, T. Lorenz, Y. Gallais, B. Fauqué, J. Hemberger, and K. Behnia, Nat. Phys. **13**, 643 (2017).

[19] K. Ahadi, L. Galletti, Y. Li, S. Salmani-Rezaie, W. Wu, and S. Stemmer, Sci. Adv. **5**, eaaw0120 (2019).

[20] X. Lin, B. Fauqué, and K. Behnia, Science **349**, 945 (2015).

[21] J. M. Edge, Y. Kedem, U. Aschauer, N. A. Spaldin, and A. V. Balatsky, Phys. Rev. Lett. **115**, 247002 (2015).

[22] D. van der Marel, F. Barantani, and C. W. Rischau, Phys. Rev. Res. **1**, 013003 (2019).

[23] C. Collignon, P. Bourges, B. Fauqué, and K. Behnia, Phys. Rev. X **10**, 031025 (2020).

[24] C. Collignon, Y. Awashima, Ravi, X. Lin, C. W. Rischau, A. Acheche, B. Vignolle, C. Proust, Y. Fuseya, K. Behnia, and B. Fauqué, Phys. Rev. Mater. **5**, 065002 (2021).

[25] A. Kumar, V. I. Yudson, and D. L. Maslov, Phys. Rev. Lett. **126**, 076601 (2021).

[26] D. E. Kiseliov and M. V. Feigel'man, Phys. Rev. B **104**, L220506 (2021).

[27] K. A. Müller, W. Berlinger, and E. Tosatti, Z. Phys. B: Condens. Matter **84**, 277 (1991).

[28] V. V. Lemanov, Ferroelectrics **265**, 1 (2002).

[29] See Supplemental Material at http://link.aps.org/supplemental/10.1103/PhysRevB.106.L140301 for the presentation of the samples, the spectrometer configurations, the experimental fitting procedure, the raw data of Fig. 1, the TO/TA phonon linewidth, and the TO dispersion [60–65].

[30] G. Shirane and Y. Yamada, Phys. Rev. **177**, 858 (1969).

[31] Y. Yamada and G. Shirane, J. Phys. Soc. Jpn. **26**, 396 (1969).

[32] P. A. Fleury, J. F. Scott, and J. M. Worlock, Phys. Rev. Lett. **21**, 16 (1968).

[33] H. Vogt, Phys. Rev. B **51**, 8046 (1995).

[34] A. A. Sirenko, C. Bernhard, A. Golnik, A. M. Clark, J. Hao, W. Si, and X. X. Xi, Nature (London) **404**, 373 (2000).

[35] D. van Mechelen, Charge and Spin Electrodynamics of SrTiO₃ and EuTiO₃ Studied by Optical Spectroscopy, Ph.D. thesis, Geneva University, 2010.

[36] R. A. Cowley and E. K. H. Salje, Philos. Trans. R. Soc., A **354**, 2799 (1996).

[37] E. V. Balashova, V. V. Lemanov, R. Kunze, G. Martin, and M. Weihnacht, Ferroelectrics **183**, 75 (1996).

[38] W. Rehwald, Solid State Commun. **8**, 1483 (1970).

[39] W. Rehwald, Solid State Commun. **8**, 607 (1970).

[40] J. Scott and H. Ledbetter, Z. Phys. B: Condens. Matter **104**, 635 (1997).

[41] B. Lüthi and T. J. Moran, Phys. Rev. B **2**, 1211 (1970).

[42] A. Laubereau and R. Zurek, Z. Naturforsch., A: Phys. Sci. **25**, 391 (1970).

[43] B. Hehlen, Z. Kallassy, and E. Courtens, Ferroelectrics **183**, 265 (1996).

[44] C. Lasota, C.-Z. Wang, R. Yu, and H. Krakauer, Ferroelectrics **194**, 109 (1997).

[45] T. Tadano and S. Tsuneyuki, Phys. Rev. B **92**, 054301 (2015).

[46] J.-J. Zhou, O. Hellman, and M. Bernardi, Phys. Rev. Lett. **121**, 226603 (2018).

[47] A. O. Fumega, Y. Fu, V. Pardo, and D. J. Singh, Phys. Rev. Mater. **4**, 033606 (2020).

[48] X. He, D. Bansal, B. Winn, S. Chi, L. Boatner, and O. Delaire, Phys. Rev. Lett. **124**, 145901 (2020).

[49] A. van Roekeghem, J. Carrete, and N. Mingo, Comput. Phys. Commun. **263**, 107945 (2021).

[50] J. D. Axe, J. Harada, and G. Shirane, Phys. Rev. B **1**, 1227 (1970).

[51] B. Hehlen, L. Arzel, A. K. Tagantsev, E. Courtens, Y. Inaba, A. Yamanaka, and K. Inoue, Phys. Rev. B **57**, R13989 (1998).

[52] E. Courtens, G. Coddens, B. Hennion, B. Hehlen, J. Pelous, and R. Vacher, Phys. Scr., T **49B**, 430 (1993).

[53] M. A. Carpenter, Am. Mineral. **92**, 309 (2007).

[54] A. Bussmann-Holder, H. Büttner, and A. R. Bishop, Phys. Rev. Lett. **99**, 167603 (2007).

[55] S. A. Ktitorov and L. Jastrabik, *The 5th Williamsburg Workshop on First-Principles Calculations for Ferroelectrics* edited by R. E. Cohen, AIP Conf. Proc. No. 436 (AIP, New York, 1998), p. 184.

[56] V. Martelli, J. L. Jiménez, M. Continentino, E. Baggio-Saitovitch, and K. Behnia, Phys. Rev. Lett. **120**, 125901 (2018).

[57] X. Li, B. Fauqué, Z. Zhu, and K. Behnia, Phys. Rev. Lett. **124**, 105901 (2020).

[58] S. Kustov, I. Liubimova, and E. K. H. Salje, Phys. Rev. Lett. **124**, 016801 (2020).

[59] G. G. Guzmán-Verri, C. H. Liang, and P. B. Littlewood, arXiv:2205.14171.

[60] T. Weber, R. Georgii, and P. Böni, SoftwareX **14**, 100667 (2021).

[61] A. Yamanaka, M. Kataoka, Y. Inaba, K. Inoue, B. Hehlen, and E. Courtens, Europhys. Lett. **50**, 688 (2000).

[62] O. Hellman, I. A. Abrikosov, and S. I. Simak, Phys. Rev. B **84**, 180301 (2011).

[63] O. Hellman, P. Steneteg, I. A. Abrikosov, and S. I. Simak, Phys. Rev. B **87**, 104111 (2013).

[64] J. P. Perdew, K. Burke, and M. Ernzerhof, Phys. Rev. Lett. **77**, 3865 (1996).

[65] G. Kresse and J. Furthmüller, Phys. Rev. B **54**, 11169 (1996).